Photocatalytic Cyclization of 2-Phosphinobiaryls to Trivalent Dibenzophospholes

Yusuke Masuda,[1]* Yu Harabuchi,[2]* Yukie Kawamura,[1] Nodoka Morooka,[1] Satoshi Maeda,[1,2] and Masaya Sawamura[1,2]*

[1] Department of Chemistry, Faculty of Science, Hokkaido University, Sapporo, Hokkaido 060-0810, Japan.

[2] Institute for Chemical Reaction Design and Discovery (WPI-ICReDD), Hokkaido University, Sapporo, Hokkaido 001-0021, Japan.

KEYWORDS: dibenzophospholes, phosphines, photoredox catalysis, mechanistic study, single electron transfer

ABSTRACT: This work demonstrates the photocatalytic cyclization of 2-phosphinobiaryls to dibenzophospholes. Using mild conditions, readily available 2-phosphinobiaryls were converted into trivalent *P*-alkyl- and *P*-aryl-dibenzophospholes. In this process, a *P*-substituent was lost from the starting phosphine in the form of a radical with preferential elimination of alkyl groups rather than aryl groups. Mechanistic experiments and quantum chemical calculations suggested that the 2-phosphinobiaryl undergoes a single electron oxidation by the excited photocatalyst to form a phosphine radical cation that then converts to the dibenzophosphole via a radical chain mechanism. Computational and experimental explorations of single electron transfer events uncovered two "hidden" radical-termination pathways, one regenerating the 2-phosphinobiaryl starting material and the other giving a phosphonium side product. These pathways explain the low quantum yield of the reaction and the need to use a photoredox catalyst with both oxidizing and reducing abilities.

INTRODUCTION

Dibenzophosphole and its derivatives have emerged as a fascinating class of organophosphorus compounds exhibiting distinctive electronic and photochemical properties, and so are promising candidates for various applications.[1–3] The properties of such compounds are known to be affected by the valency of the phosphorus atom and by the specific substituents.[4] In particular, it would be desirable to devise methods for the synthesis of trivalent dibenzophospholes that enable facile modification of the phosphorus center. At present, these compounds are typically synthesized via the nucleophilic substitution reactions of dichlorophosphines with 2,2'-dilithiobiaryls generated by halogen-lithium exchange with the corresponding dihalobiaryls and alkyllithium reagents.[5] In contrast, the cyclization of 2-phosphinobiaryls[6–9] through direct C–H functionalization could potentially allow the synthesis of dibenzophospholes. Available C–H activation methods were applied solely to the production of pentavalent dibenzophosphole derivatives such as phosphole oxides[10–17] and phospholanium salts[18–21] until Tobisu and Chatani introduced the palladium-catalyzed cyclization of 2-(diarylphosphino)biaryls based on a C–H/P–Ar double activation as a means of synthesizing trivalent dibenzophospholes (Figure 1a and 1b).[22] Even so, the construction of *P*-alkyldibenzophospholes using this palladium-catalyzed approach requires a phosphine with three different *P*-substituents as a starting material and thus far only a single example of this process has been reported.

During our work on developing new reactions for the molecular-editing of tertiary phosphines,[23–27] the photocatalytic cyclization reactions of 2-phosphinobiaryls were found to produce dibenzophospholes (Figure 1c). In contrast to the palladium-catalyzed method, this process is applicable to 2-*P*,*P*-diorganobiaryls having alkyl or aryl substituents on the phosphorous atom of the diorganophosphino core. Hence, a range of structurally diverse *P*-alkyl- and *P*-aryl-dibenzophospholes can potentially be obtained.

Photoredox catalysis has brought about a renaissance in synthetic organic chemistry. However, the underlying reaction mechanisms involving single-electron transfer pathways remain elusive. In the present work, we tackled this issue with a comprehensive mechanistic investigation through a combined approach of computational and experimental studies. As a result, a radical-chain mechanism initiated by the single electron oxidation of the starting phosphine was suggested for the photocatalytic cyclization of diorganophosphinobiaryls to the corresponding trivalent dibenzophospholes. Additional computational and experimental exploration uncovered two off-cycle chain termination pathways respectively giving the original 2-phosphinobiaryl and a phosphonium side product. In this process, the photocatalyst both oxidizes the starting substrate to initiate the radical chain reaction and reduces the phosphonium side product such that it reenters the radical chain reaction cycle.

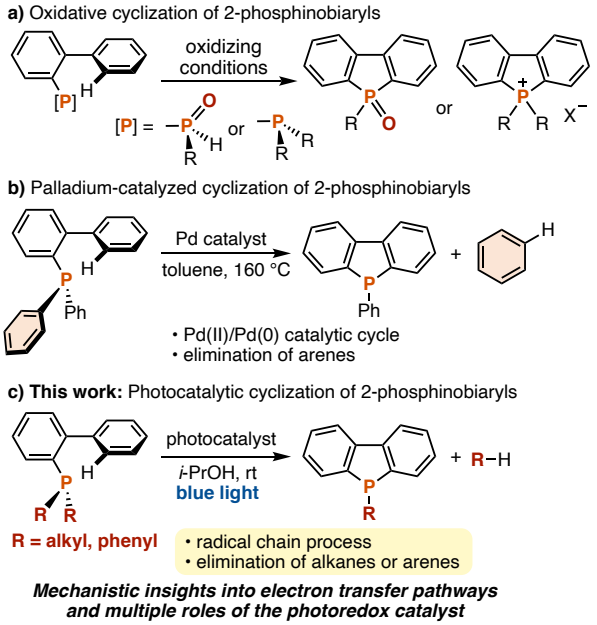

Figure 1. Cyclization of 2-phosphinobiaryls to dibenzophosphole derivatives. (a) Oxidative cyclization. (b) The palladium-catalyzed approach. (c) The photocatalytic approach (this work).

METHODS

Typical procedure for the synthesis of 4a. To an oven-dried 4 mL vial equipped with a stirrer bar, **Ir1** (1.1 mg, 0.001 mmol, 1.0 mol%) and 2-phosphinobiaryl **1a** (29.8 mg, 0.10 mmol) were added. The vial was purged with argon gas and was taken into a nitrogen-filled glove box. In the glove box, isopropyl alcohol (1.0 mL) was added to the vial. The vial was capped and taken out of the glove box, and the solution was stirred under photoirradiation (470 nm) at ambient temperature for 15 h. After irradiation, the solvent was removed under reduced pressure. Acetone (1 mL) and a few drops of an aqueous solution of H_2O_2 (ca. 30%) were sequentially added to the residue, and the mixture was stirred at room temperature for 0.5 h. Then, the resulting mixture was concentrated under reduced pressure. The crude mixture was purified by preparative thin-layer chromatography (CH_2Cl_2/CH_3OH = 97:3) to give **4a** as white solids (20.0 mg, 0.078 mmol, 78% yield).

RESULTS AND DISCUSSION

Reaction Development. Initial work employed the commercially available compound 2-(di-*t*-butylphosphino)biphenyl (**1a**), otherwise known as a Buchwald-type JohnPhos ligand,[28] as the starting substrate. In these trials, a solution of **1a** (0.1 M) was irradiated with blue light-emitting diodes (LEDs, 470 nm) in the presence of the photocatalyst $[Ir(dFCF_3ppy)_2dtbbpy]PF_6$ (**Ir1**, 1 mol%) at ambient temperature for 15 h. The resulting yield of dibenzophosphole **2a** was determined by analysis of the crude reaction mixture using ^1H NMR. The reaction in toluene afforded a small amount of **2a** (10%) but the majority of the starting phosphine was recovered (Table 1, entry 1). The use of more polar solvents such as acetonitrile (CH_3CN) and tetrahydrofuran (THF) improved the yield of **2a** (entries 2 and 3). Further screening of solvents revealed that protic solvents were best suited to this process. The reaction in methanol (CH_3OH) afforded the target product (**2a**) in an 83% yield (entry 4). Finally, isopropyl alcohol (*i*-PrOH) was found to be the most effective, giving **2a** in a 93% yield (entry 5).

Table 1. Optimization of the photocatalytic cyclization reaction of 2a.[a]

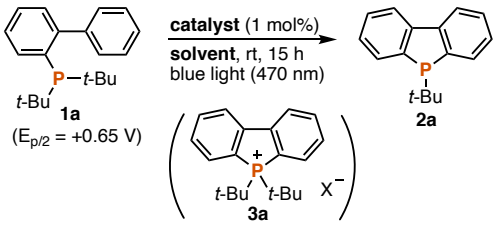

entry	catalyst	solvent	yield of **2a**
1	**Ir1**	toluene	10%
2	**Ir1**	CH_3CN	40%
3	**Ir1**	THF	56%
4	**Ir1**	CH_3OH	83%
5	**Ir1**	*i*-PrOH	93%
6	**Ir2**	*i*-PrOH	96%
7	**Ir3**	*i*-PrOH	0%
8	**Ir4**	*i*-PrOH	5%[b]

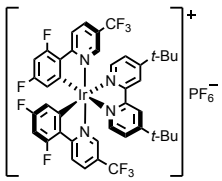

$[Ir(dFCF_3ppy)_2dtbbpy]PF_6$
(**Ir1**)
$E_{1/2}(Ir^{III*}/Ir^{II})$: **+1.21 V**
$E_{1/2}(Ir^{III}/Ir^{II})$: –1.37 V

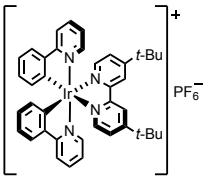

Ir2
$E_{1/2}(Ir^{III*}/Ir^{II})$: **+0.66 V**
$E_{1/2}(Ir^{III}/Ir^{II})$: –1.51 V

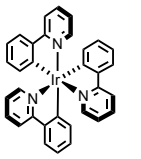

Ir3
$E_{1/2}(Ir^{III*}/Ir^{II})$: **+0.35 V**
$E_{1/2}(Ir^{III}/Ir^{II})$: –2.19 V

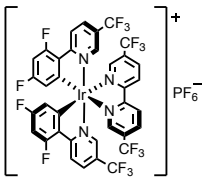

Ir4
$E_{1/2}(Ir^{III*}/Ir^{II})$: **+1.68 V**
$E_{1/2}(Ir^{III}/Ir^{II})$: –0.69 V

[a] **1a** (0.10 mmol), catalyst (0.001 mmol, 1 mol%), solvent (1 mL), blue LEDs (470 nm), rt, 15 h. Yields determined by ^1H NMR using 1,1,2,2-tetrachloroethane as an internal standard. [b] A 7% yield of **3a** was observed.

A series of iridium photocatalysts having different redox characteristics was subsequently examined. Photocatalyst **Ir2** [$E_{1/2}$ (Ir^{III*}/Ir^{II}) = +0.66 V vs SCE in CH_3CN][29] produced **2a** in a yield comparable to that obtained using **Ir1** [$E_{1/2}$ (Ir^{III*}/Ir^{II}) = +1.21 V vs SCE in CH_3CN][30] whereas the reaction did not proceed with the weakly oxidizing catalyst **Ir3** [$E_{1/2}$ (Ir^{III*}/Ir^{II}) = +0.35 V vs SCE in CH_3CN][31] (Table 1, entries 6 and 7). Considering the oxidation potential of **1a** ($E_{p/2}$ = +0.65 V vs SCE in CH_3CN), these results suggested that electron transfer from **1a** to the excited photocatalyst

was involved in the reaction mechanism. Product **2a** showed a higher oxidation potential ($E_{p/2}$ = +1.43 V vs SCE in CH_3CN), indicating that product oxidation is unlikely to occur under these reaction conditions. It should also be noted that the use of the strongly oxidizing catalyst **Ir4** [$E_{1/2}$ (Ir^{III*}/Ir^{II}) = +1.68 V vs SCE in CH_3CN][32] resulted in a very low conversion of the starting phosphine and gave phosphonium salt **3a** as a side product (entry 8).

Derivatization of Dibenzophosphole. The product **2a** could be derivatized to produce various other compounds through modification at the phosphorus atom (Scheme 1). As an example, treatment of crude **2a** with an aqueous solution of hydrogen peroxide (H_2O_2) afforded phosphine oxide **4a** in a 78% yield. Phosphine sulfide **5a** and phosphonium salt **6a** were also synthesized in trials using elemental sulfur (S_8) and methyl iodide (MeI), respectively. In addition, treatment with BH_3·THF provided the borane adduct (**7a**) in a 71% yield.

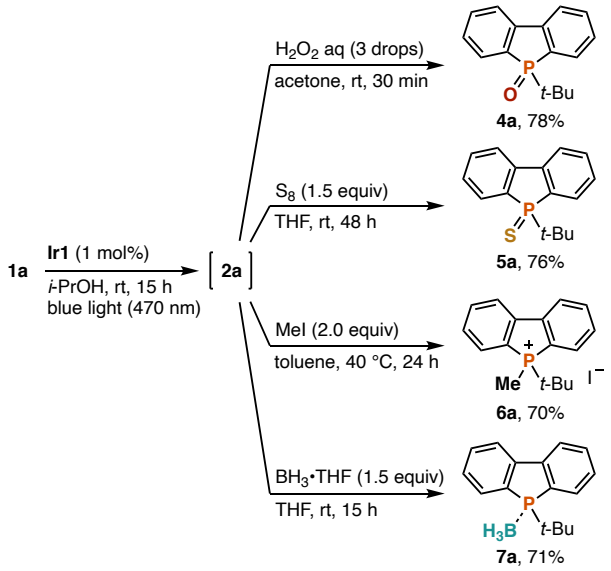

Scheme 1. Derivatization of 2a.

Substrate Scope. Various 2-phosphinobiaryls were also applied to the present photocyclization reaction. The presence of secondary alkyl moieties such as isopropyl and cyclohexyl groups as *P*-substituents on the 2-(*P,P*-dialkylphosphino)biphenyl was found to be tolerated and the corresponding *P*-alkyldibenzophosphole oxides (**4b** and **4c**) were obtained in 88% and 77% yields, respectively, after oxidation of the trivalent phospholes. In contrast, *P,P*-diethylphosphinobiphenyl reacted more slowly, affording the cyclized product **4d** in a moderate yield. The reaction also proceeded in the case that *P,P*-diphenylphosphinobiphenyl (**1e**) was employed, producing dibenzophosphole **4e** via the elimination of one of the phenyl groups. Thus, both *P*-alkyl and *P*-phenyl substituents could be eliminated during the present photocatalytic reaction. This process is evidently superior to existing palladium-catalyzed reactions in which only aryl moieties can function as leaving groups. The effects of the substituent on the terminal phenyl ring of the starting phosphinobiaryl were also examined. Substrates having one or more methyl groups at the *para*, *ortho* or *meta* positions of the terminal phenyl ring were found to participate in this reaction (**4f**–**4h**). The presence of a fluorine atom also did not affect the reaction efficiency (**4i**) whereas a C–Cl bond was found to be labile, undergoing dehalogenative decomposition under these reaction conditions (**4j**). Electron-withdrawing functional moieties such as trifluoromethyl, cyano and amide groups were all tolerated (**4k**, **4l** and **4m**). The reaction also proceeded with electron-donating methoxy and 4-carbazoyl groups on the starting phosphinobiaryl (**4n** and **4o**). Finally, this technique could be used to synthesize dibenzophospholes having extended π-systems (**4p**, **4q** and **4r**).

Using the same substrates, the resulting dibenzophospholes could also be isolated as borane complexes through reaction with BH_3·THF. Borane complexes **7b**, **7f**, **7i**, **7k**, **7o** and **7p** were obtained in yields comparable to those of the corresponding phosphine oxides, demonstrating the practicality of this method for synthesizing trivalent dibenzophospholes.

The reaction of a phosphinobiphenyl bearing a methyl group at the *meta* position of the terminal phenyl ring (**1s**), which had two possible sites for C–P bond formation, afforded a mixture of **4s** and **4s'** in 44% yields with no site-selectivity (**4s**/**4s'** 50:50). In contrast, a substrate with a 9-carbazoyl substituent at the *meta* position (**1t**) gave the corresponding products (**4t** and **4t'**) in a ratio of 62:38, suggesting that the electronic properties of *meta*-substituent can affect the site-selectivity of the cyclization.

Dibenzophosphole derivatives with electron-donating substituents are expected to function as photoluminescent materials.[33] Thus, the optical properties of the carbazole-substituted dibenzophospholes produced in this work (**4o**, **4t** and **4t'**) were assessed. Although all these compounds produced similar emission spectra (λ_{max} = 425, 422 and 432 nm, respectively), **4t'** showed significantly weaker luminescence compared with the other compounds (See Supporting Information for details). This outcome is ascribed to the lack of effective conjugation between the dibenzophosphole ring and the carbazolyl group in **4t'**.

When the reaction was conducted with a phosphinobiphenyl possessing *t*-butyl and phenyl groups as two different *P*-substituents (**1u**), the *t*-butyl group was preferentially eliminated such that only *P*-phenyldibenzophosphole **4e** was produced. We assumed that a *P*-substituent was lost from the starting phosphine in the form of a radical with preferential elimination of a *t*-butyl group rather than a phenyl group. This result is in contrast to the selective P–C(phenyl) bond cleavage that occurs in the case of the palladium-catalyzed reaction to give a *P*-alkyl dibenzophosphole.[22]

Table 2. Substrate scope.[a]

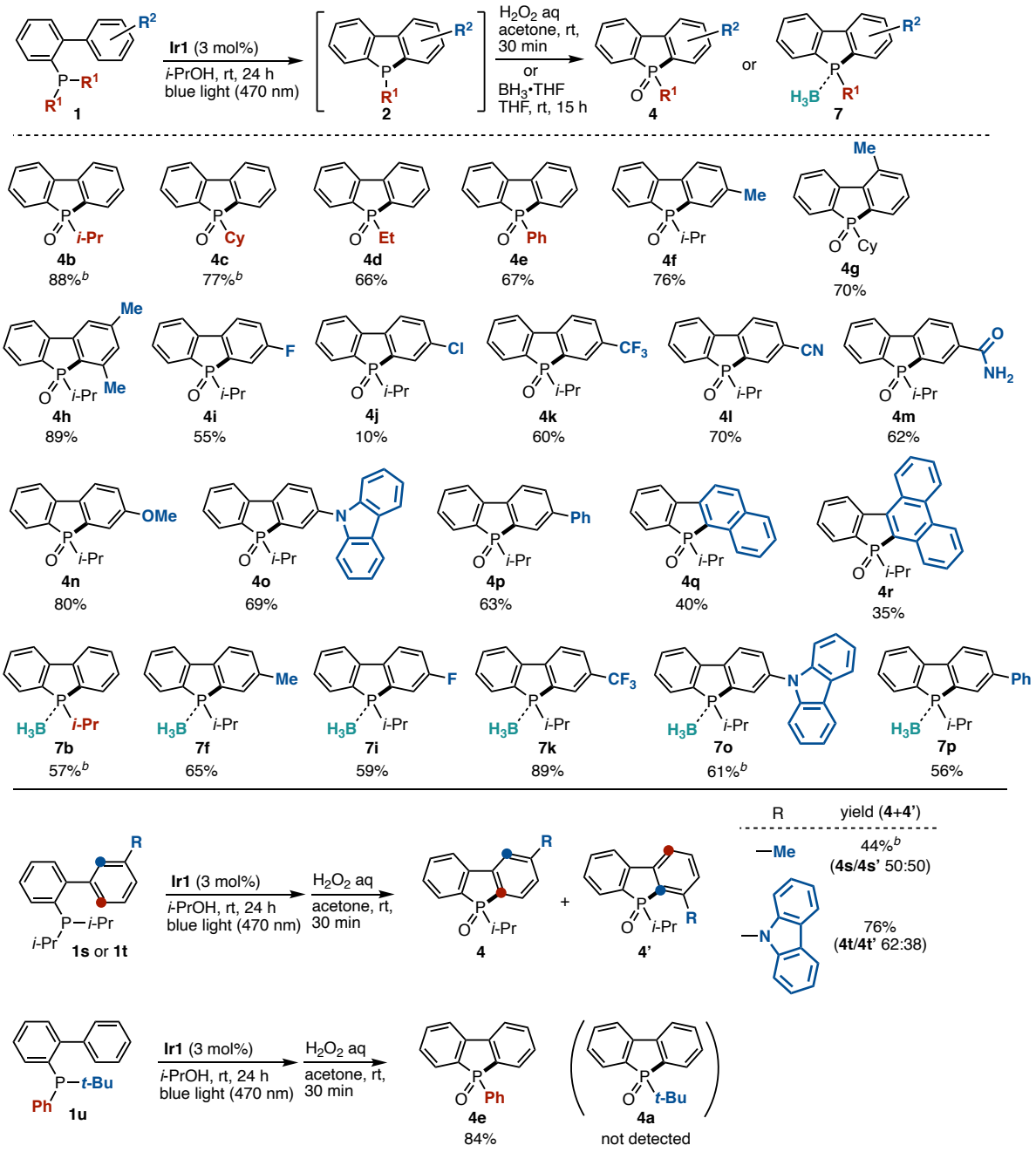

[a] 1) **1** (0.10 mmol), **Ir1** (0.003 mmol, 3 mol%), *i*-PrOH (1 mL), blue LEDs (470 nm), rt, 24 h; 2) For phosphine oxide: H_2O_2 (several drops of a 30% aqueous solution), acetone (1 mL), rt, 30 min. For phosphine-borane: BH_3·THF (1.5 equiv), THF (1 mL), rt, 15 h. Isolated yields are shown. [b] **Ir1** (0.001 mmol, 1 mol%), 15 h.

Synthetic Applications. The reaction was scalable. When a 1 mmol quantity of **1a** was used, trivalent dibenzophosphole **2a** was obtained in 96% yield simply by extraction from a crude residue with hexane (Scheme 2a). The 2-phosphinobiaryl moiety is a privileged molecular framework found in Buchwald-type phosphine ligands.[28] The present protocol was found to transform bis(2-biphenyl)-*t*-butylphosphane (**1v**)[34] directly into a new Buchwald-type ligand (**2v**) featuring a dibenzophosphole as the coordination site (Scheme 2b). This product was found to be sufficiently stable in air to be isolated in the form of a trivalent phosphine. The complexation of a gold precursor with the phosphine ligand **2v** took place, forming gold complex **2v·AuCl** in quantitative yield.

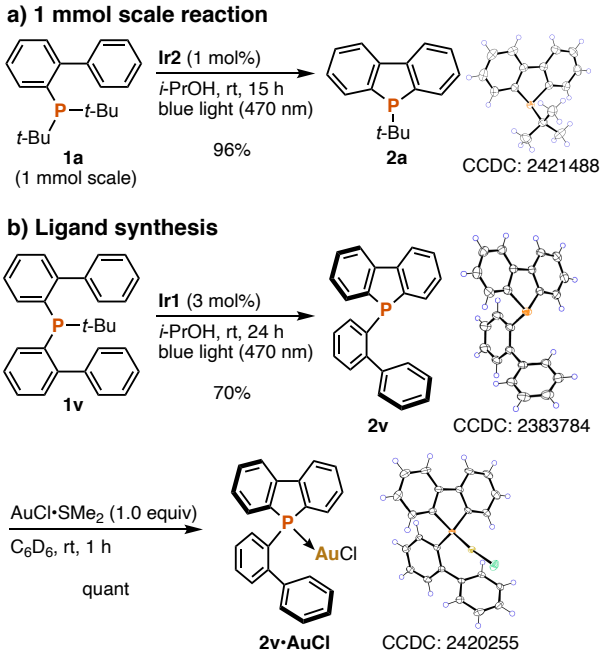

Scheme 2. Synthetic applications.

Mechanistic Experiments. Subsequent to the above, the reaction was performed in a sealed NMR tube to allow the analysis of volatile byproducts. A trial using **1a** in deuterated acetonitrile (CD_3CN) generated isobutane (*t*-Bu–H) along with **2a** (Scheme 3a). In contrast, a reaction in methanol-d_4 (CD_3OD) yielded isobutane deuterated at the methine carbon (*t*-Bu–D, >95% D) (Scheme 3b). It was also found that the reaction proceeded much more rapidly in methanol than in acetonitrile. The use of CD_3OH resulted in the formation of non-deuterated isobutane (*t*-Bu–H) (Scheme 3c), indicating that the hydrogen atom at the methine carbon of the isobutane was derived from the hydroxy group of the alcoholic solvent.

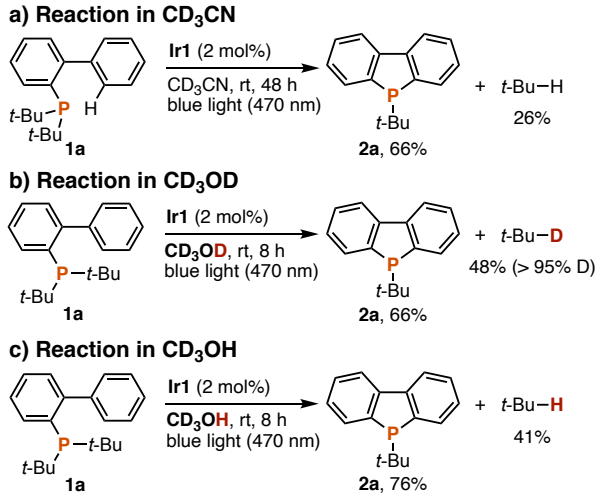

Scheme 3. Mechanistic Experiments.

The results detailed above suggested that the *P*-substituent of the phosphine substrate was eliminated as a radical species on the basis of homolytic C–P bond cleavage. To test this hypothesis, the reaction of 2-(di-*t*-butylphosphino)biphenyl (**1a**) was conducted in the presence of activated alkenes intended to trap any eliminated *tert*-butyl radicals via C–C bond formation (Scheme 4). The irradiation of a 1:1 mixture of **1a** and benzyl acrylate with blue LEDs in the presence of photocatalyst **Ir1** gave the expected *tert*-butylated product **8** in an 87% yield along with the quantitative formation of **2a**. The *tert*-butylated product was also obtained in a trial with diisopropyl fumarate and with the electronically neutral 1,1-diphenylethylene, affording **9** and **10**, respectively. These observations provided support for the formation of *t*-butyl radical species as intermediates.

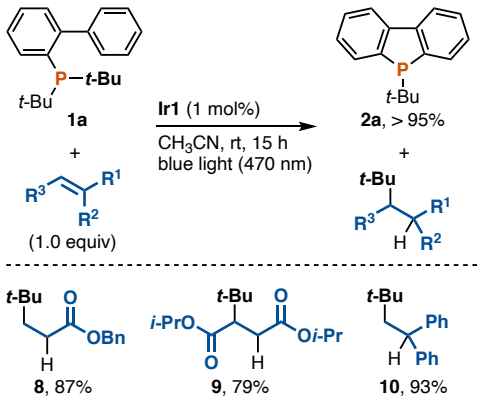

Scheme 4. Photocatalytic reactions of 1a with alkenes.

Computational Study. Quantum chemical calculations were also carried out to model the reaction forming dibenzophosphole **2a**, working at the ωB97X-D/6-31+G(d,p)/SMD(CH_3OH) level of theory with an empirical correction for translational and rotational entropies[35] (Figure 2a). The results confirmed the feasibility of a radical chain reaction mechanism initiated with phosphine radical cation **A**. In this process, **A** is generated via the single-electron oxidation of **1a** by the excited state photocatalyst.[36] This cation (0.0 kcal mol^{-1}, all other Gibbs free energies are relative to this point) then undergoes a facile 5-*endo-trig* cyclization and appends to the terminal phenyl ring to form cyclohexadienyl radical species **B** (–8.7 kcal mol^{-1}) with a free energy barrier of 4.0 kcal mol^{-1} (**TS₁**). The proton of **B** adjacent to the phosphorous atom subsequently undergoes a solvent-mediated abstraction by another molecule of **1a** through trimolecular transition state **TS₂** (10.7 kcal mol^{-1}). In this manner, the electronically neutral radical species **C** with pseudo C_{2v} symmetry is generated along with the protonated phosphine (**1a·H⁺**) (–11.1 kcal mol^{-1}). The direct transfer of a proton from **B** to **1a** involves a higher activation energy of 24.4 kcal mol^{-1}, which explains why the reaction was accelerated when performed in an alcohol. The spin density, originally localized at one of the two six-membered rings of the cyclohexadienyl radical intermediate **B**, is equally delocalized on the two benzene rings in **C** (Figure 2b). One of the C(sp^3)–P bonds of **C** then becomes elongated until a *t*-butyl radical (*t*-Bu•) is lost in conjunction with the formation of a van

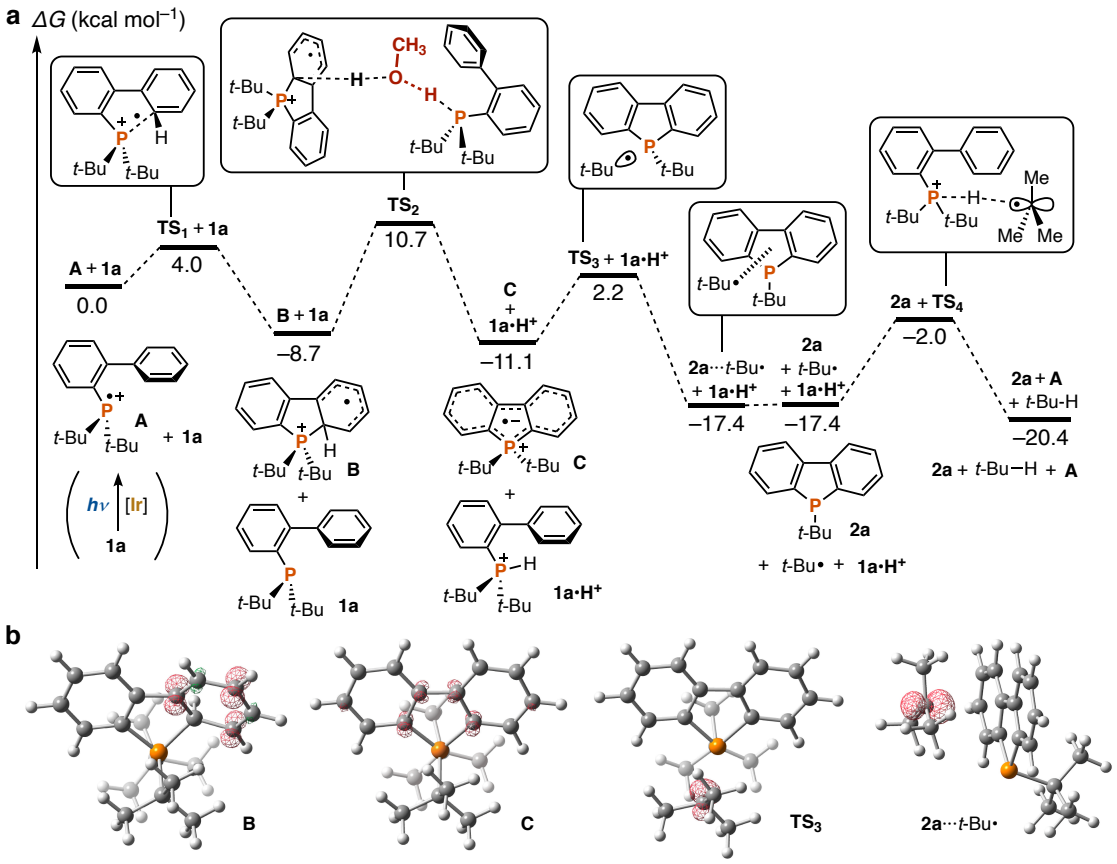

Figure 2. (a) Energy diagrams calculated at the ωB97X-D/6-31+G(d,p)/SMD(CH_3OH) level. All Gibbs free energies, incorporating an empirical correction for translational and rotational entropies,[17] are relative to **A** + **1a** + methanol and are in kcal mol^{-1} (see Supporting Information). Methanol molecules are omitted in the figure. (b) Spin densities of selected intermediates and transition state (indicated by the red mesh).

der Waals complex with **2a** (**2a**···*t*-Bu•, −17.4 kcal mol^{-1}).[37,38] This process involves a free energy barrier of 13.3 kcal mol^{-1}. The decomplexation of **2a**···*t*-Bu• affords **2a** and a *t*-butyl radical (*t*-Bu•) with a tiny change in free energy. The *t*-butyl radical then accepts a hydrogen atom from the protonated phosphine (**1a·H⁺**) to afford isobutane (*t*-Bu–H) with the concurrent regeneration of **A**. All the elementary steps in this process are exergonic, with a total stabilization energy (the energy difference between **1a** and **2a**+*t*-Bu–H) as high as 20.4 kcal mol^{-1}.

The formation of *t*-Bu–D during the reaction using CD_3OD as the solvent (Scheme 3b) can be explained as follows. When the reaction is carried out in CD_3OD, a deuterium atom is attached to the phosphorus atom to give **1a·D⁺** via a solvent-mediated proton transfer (**TS₂**-d_4). This deuterium is eventually abstracted by a *t*-butyl radical (*t*-Bu•) to produce the deuterated isobutane (*t*-Bu–D).

Although the computational studies provided a mechanism for the radical chain pathway, the quantum yield of the photocatalytic reaction of **1a** was determined to be just 0.1 using potassium ferrioxalate as an actinometer (Scheme 5).[39,40] This low quantum yield suggested the possibility of radical termination pathways in the reaction mechanism. For this reason, the likelihood of single electron transfer (SET) events aside from the radical chain reaction cycle was assessed.

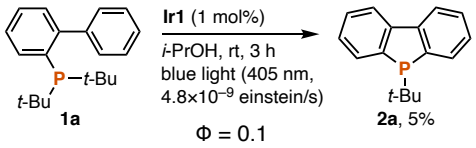

Scheme 5. Quantum yield (Φ) of the photocatalytic cyclization reaction.

The SET processes occurring between a photoredox catalyst and substrates/intermediates can involve a crossing of potential energy surfaces,[41–49] equivalent to the seam of crossing (SX) in the Marcus theory.[50–55] In this work, possible SET events proceeding through SXs were examined using a computational approach[56] based on the energy-shift method[57,58] implemented in the GRRM program.[59] Specifically, minimum energy SXs were explored for all the calculated structures shown in Figure 2 over the potential energy range from −2.0 V (55.9 kcal mol^{-1}) to +1.0 V (125.0 kcal mol^{-1}) (see Supporting Information for details). The reduction potential for the **Ir1** photocatalyst that was experimentally determined to be optimal [− 1.37 V (70.4 kcal mol^{-1})] exhibited a minimum energy SX near the structure of radical cation **B** (with a calculated electronic energy barrier of < 0.1 kcal mol^{-1}). This finding indicated that a SET from the reduced state photocatalyst (**[Ir^{II}]**) to **B** can occur to give cyclohexadienyl anion **D** along with the photocatalyst in the ground state (**[Ir^{III}]⁺**), thus terminating the

radical chain process (Scheme 6a). Following this step, **D** spontaneously undergoes a ring-opening reaction to regenerate **1a,** with a low Gibbs energy barrier (2.6 kcal mol^{-1}).

The additional computational exploration of SET pathways indicated that **B** could also be reduced by **C** to produce phosphonium salt **3a** and **D** without regeneration of the photocatalyst. This involves a calculated Gibbs energy barrier of 3.0 kcal mol^{-1} (Scheme 6b).[60]

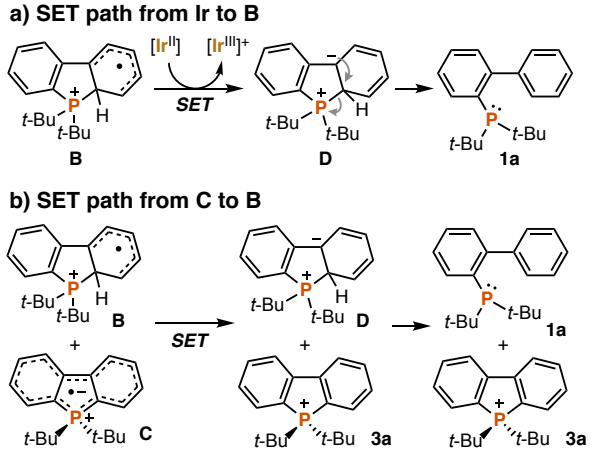

Scheme 6. Predicted SET pathways.

Experimental Supports for SET Pathways. To obtain experimental support for the formation of the zwitterionic species **D** as an intermediate, the protonating photocatalytic reaction of phenanthrene-substituted phosphine **1r** was performed (Scheme 7). This process was expected to generate a more stable zwitterionic intermediate. In this experiment, a solution of **1r** was irradiated in the presence of **Ir1** and ammonium tetrafluoroborate as a proton source. Phosphonium salt **11** was obtained in a 45% yield as the primary product and the molecular structure of this compound was unambiguously determined by single crystal X-ray diffraction (CCDC: 2365577). This outcome suggested that **D** was formed during the catalytic process.

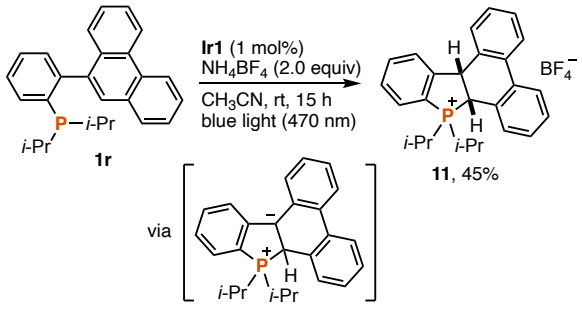

Scheme 7. Protonation trapping of the dearomatized intermediate.

If the electron transfer process converting **C** to **3a** that is shown in Scheme 6b occurs, the photocatalytic reaction would be expected to terminate prematurely because it does not regenerate the ground state photocatalyst (**[Ir^{III}]**$^{+}$). The fact that the reaction proceeded to completion with the appropriate catalyst implies the existence of a pathway that allows **3a** to reenter the radical chain process (see Scheme 8). Consequently, the likelihood of this backward reaction, meaning the reduction of **3a** to **C**, was investigated using a reduced state photocatalyst (**[Ir^{II}]**). This photocatalyst could be generated in situ by a reaction with an amine reductant. In these trials, a mixture of **3a·BF$_4$** ($E_{p/2}$ = –1.60 V vs SCE in CH_3CN) and benzyl acrylate was irradiated with blue LEDs in the presence of a photocatalyst and *N,N*-diisopropylethylamine (*i*-Pr_2NEt) as a reductant (Table 3). The catalysts **Ir1**, **Ir2** and **Ir3** were all found to reduce **3a·BF$_4$** to phosphine **2a** under these conditions.[61–68] The *t*-butyl radical eliminated in each experiment was then trapped by the alkene to form **8** (Table 3, entries 1–3). In contrast, the weakly reducing catalyst **Ir4** [$E_{1/2}$(Ir^{III}/Ir^{II}) = –0.69 V vs SCE in CH_3CN] failed to give **2a** and the original **3a·BF$_4$** could be recovered (entry 4). This outcome was consistent with the observation that **Ir4** was an inefficient catalyst for the formation of dibenzophospole **2a** and instead gave the phosphonium side product **3a** (Table 1, entry 8). These results suggested that a photocatalyst possessing sufficient reducing ability was required to bring **3a** back into the radical chain process.

Table 3. Effects of various photocatalysts on the reduction of 3a.[a]

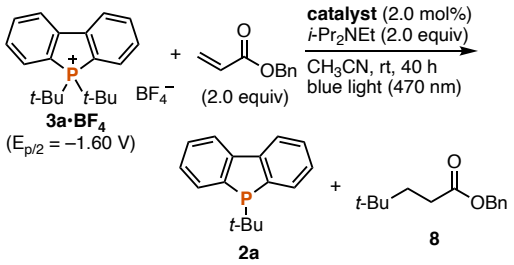

entry	catalyst	$E_{1/2}$ Ir^{III}*/Ir^{II}	$E_{1/2}$ Ir^{III}/Ir^{II}	yield of **2a**	yield of **8**
1	**Ir1**	1.21 V	**–1.37 V**	53%	42%
2	**Ir2**	0.66 V	**–1.51 V**	92%	39%
3	**Ir3**	0.35 V	**–2.19 V**	92%	33%
4	**Ir4**	1.68 V	**–0.69 V**	0%	0%

[a] **3a·BF$_4$** (0.10 mmol), catalyst (0.002 mmol, 2 mol%), benzyl acrylate (0.20 mmol, 2.0 equiv), *i*-Pr_2NEt (0.20 mmol, 2.0 equiv), CH_3CN (1 mL), blue LEDs (470 nm), rt, 40 h. Yields determined by ^{1}H NMR using 1,1,2,2-tetrachloroethane as an internal standard.

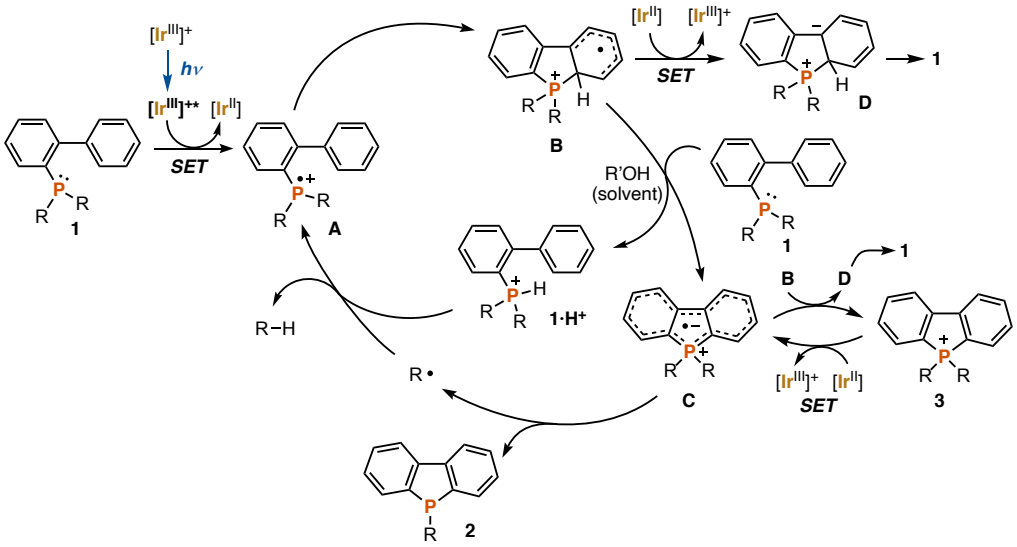

Scheme 8. Proposed reaction mechanism.

Proposed Mechanism. Based on the results of the experimental and computational mechanistic studies detailed above, a mechanism for the photocatalytic reaction of 2-(dialkylphosphino)biaryls (**1**) to produce dibenzophospholes (**2**) was developed, as shown in Scheme 8. In this mechanism, the photocatalyst (**[Ir^{III}]$^+$**) is initially excited by photoirradiation and the excited compound (**[Ir^{III}]$^{+*}$**) subsequently oxidizes the starting phosphine (**1**) to generate phosphine radical cation **A** along with the transition of the photocatalyst to the reduced state (**[Ir^{II}]**). Radical cation **A** then undergoes 5-*endo-trig* cyclization to form dearomatized intermediate **B**. Following this, the deprotonation of **B** with phosphine **1** occurs, mediated by the alcoholic solvent, affording the reduced dibenzophospholanium **C** along with the protonated phosphine **1·H$^+$**. The electronically neutral intermediate **C** subsequently loses a substituent from the phosphorous atom in the form of a carbon radical (R•) to furnish dibenzophosphole **2**. Finally, the transfer of a hydrogen atom from **1·H$^+$** to R• gives a hydrocarbon byproduct (R–H) along with another phosphine radical cation **A**. This radical chain process can be terminated by two major SET events. One is the single-electron reduction of the dearomatized intermediate **B** by the reduced state of the photocatalyst (**[Ir^{II}]**), giving rise to cyclohexadienyl anion **D**. Following this, **D** spontaneously undergoes ring opening to regenerate the starting phosphine **1**. The other pathway involves a SET from electronically neutral radical species **C** to radical cation **B** to furnish phospholanium **3** and **D**. Phospholanium salt **3** then receives a single electron from the photocatalyst in the reduced state (**[Ir^{II}]**) and reenters the radical chain process as intermediate **C** along with the regeneration of the ground-state photocatalyst (**[Ir^{III}]$^+$**).

CONCLUSIONS

The photocatalytic cyclization of 2-phosphinobiaryls to trivalent dibenzophospholes was developed. This reaction proceeded under simple conditions and afforded a variety of *P*-alkyl- and *P*-aryldibenzophospholes that could be directly derivatized through modification at their trivalent phosphorus atoms. A series of mechanistic experiments and theoretical calculations suggested that this reaction mechanism is initiated by the single-electron oxidation of the starting phosphine by the photoexcited catalyst. It also appears that the phosphine radical cation generated in this reaction is converted into the dibenzophosphole through a radical chain mechanism. Calculations based on the energy-shift method further revealed that this radical chain process is accompanied by two radical-terminating electron transfer reactions that respectively regenerate the starting phosphine and produce a phosphonium side product. These computational results combined with additional mechanistic experiments explain the low quantum yield of the reaction and the necessity of a photoredox catalyst with both oxidizing and reducing abilities. This work demonstrates the utility of the quantum chemical mechanism elucidation in the study of photoredox catalysis.

AUTHOR INFORMATION

Corresponding Author

ymasuda@sci.hokudai.ac.jp (Y.M.)
y_harabuchi@icredd.hokudai.ac.jp (Y.H.)
sawamura@sci.hokudai.ac.jp (M.S.)

Funding Sources

This work was supported by JSPS KAKENHI Grants-in-Aid for Scientific Research (C) (YM; grant no. JP23K04728), Scientific Research (B) (YH; grant no. JP23K26647), Transformative Research Area (A) Digitalization-driven Transformative Organic Synthesis (Digi-TOS) (YM; grant no. JP24H01047) and Challenging Research (Exploratory) (YM, YH; grant no. JP22K19002). Funding was also obtained from the Japan Science and Technology Agency (JST) ERATO (SM; grant no. JPMJER1903) and FOREST programs (YH; grant no. JPMJFR2221) and from the Astellas Foundation for Research on Metabolic Disorders (YM) and the Uehara Memorial Foundation (YM).

Notes

The authors declare no competing financial interest.

ASSOCIATED CONTENT

Supporting Information

The Supporting Information is available free of charge on the ACS Publications website.

Experimental procedures, details of mechanistic studies, computational details, compound-characterization data for all new compounds, and NMR spectra (PDF).
Optimized Cartesian coordinates (xyz).
Crystal structure of **2a** (cif).
Crystal structure of **2v** (cif).
Crystal structure of **2v•AuCl** (cif).
Crystal structure of **11** (cif).

ACKNOWLEDGMENT

We thank the Open Facility, Global Facility Center, Creative Research Institution for carrying out the mass spectrometry analyses. Some of the calculations reported herein were performed at the Computer Center of Kyoto University and using the supercomputer system at the Information Initiative Center in Hokkaido University.

REFERENCES

(1) Baumgartner, T. Insights on the Design and Electron-Acceptor Properties of Conjugated Organophosphorus Materials. *Acc. Chem. Res.* **2014**, *47*, 1613–1622.

(2) Duffy, M. P.; Delaunay, W.; Bouit, P.-A.; Hissler, M. π-Conjugated phospholes and their incorporation into devices: components with a great deal of potential. *Chem. Soc. Rev.* **2016**, *45*, 5296–5310.

(3) Hibner-Kulicka, P.; Joule, J. A.; Skalika, J.; Bałczewski, P. Recent studies of the synthesis, functionalization, optoelectronic properties and applications of dibenzophospholes. *RSC Adv.* **2017**, *7*, 9194–9236.

(4) Matano, Y.; Imahori, H. Design and synthesis of phosphole-based π systems for novel organic materials. *Org. Biomol. Chem.* **2009**, *7*, 1258–1271.

(5) Wittig, G.; Maercker, A. Zur Reaktionsweise aromatischer Spirophosphorane. *Chem. Ber.* **1964**, *97*, 747–768.

(6) Baba, K.; Tobisu, M.; Chatani, N. Palladium-Catalyzed Synthesis of Six-Membered Benzofuzed Phosphacycles via Carbon–Phosphorus Bond Cleavage. *Org. Lett.* **2015**, *17*, 70–73.

(7) Lian, Z.; Bhawal, B. N.; Yu, P.; Morandi, B. Palladium-catalyzed carbon-sulfur or carbon-phosphorus bond metathesis by reversible arylation. *Science* **2017**, *356*, 1059–1063.

(8) Baba, K.; Masuya, Y.; Chatani, N.; Tobisu, M. Palladium-catalyzed Cyclization of Bisphosphines to Phosphacycles via the Cleavage of Two Carbon–Phosphorus Bonds. *Chem. Lett.* **2017**, *46*, 1296–1299.

(9) Fujimoto, H.; Kusano, M.; Kodama, T.; Tobisu, M. Cyclization of Bisphosphines to Phosphacycles via the Cleavage of Two Carbon–Phosphorus Bonds by Nickel Catalysis. *Org. Lett.* **2019**, *21*, 4177–4181.

(10) Kuninobu, Y.; Yoshida, T.; Takai, K. Palladium-Catalyzed Synthesis of Dibenzophosphole Oxides via Intramolecular Dehydrogenative Cyclization. *J. Org. Chem.* **2011**, *76*, 7370–7376.

(11) Furukawa, S.; Haga, S.; Kobayashi, J.; Kawashima, T. Synthesis of π-Extended Dibenzophospholes by Intramolecular Radical Cyclization and Their Properties. *Org. Lett.* **2014**, *16*, 3228–3231.

(12) Cui, Y.; Fu, L.; Cao, J.; Deng, Y.; Jiang, J. Synthesis of Dibenzophosphole Oxides via Palladium-Catalyzed Intramolecular Direct Arylation Reactions of ortho-Halodiarylphosphine Oxides. *Adv. Synth. Catal.* **2014**, *356*, 1217–1222.

(13) Nishimura, K.; Hirano, K.; Miura, M. Synthesis of Dibenzophospholes by Tf_2O-Mediated Intramolecular Phospha-Friedel–Crafts-Type Reaction. *Org. Lett.* **2019**, *21*, 1467–1470.

(14) Berger, O.; Montchamp, J. L. Manganese-Catalyzed and Mediated Synthesis of Arylphosphinates and Related Compounds. *J. Org. Chem.* **2019**, *84*, 9239–9256.

(15) Fujimoto, H.; Kusano, M.; Kodama, T.; Tobisu, M. Aryne-Induced S_NAr/Dearylation Strategy for the Synthesis of Fluorinated Dibenzophospholes from Triarylphosphines via a P(V) Intermediate. *Org. Lett.* **2020**, *22*, 2293–2297.

(16) Nishimura, K.; Hirano, K.; Miura, M. Direct Synthesis of Dibenzophospholes from Biaryls by Double C–P Bond Formation via Phosphenium Dication Equivalents. *Org. Lett.* **2020**, *22*, 3185–3189.

(17) Kurimoto, Y.; Yamashita, J.; Mitsudo, K.; Sato, E.; Suga, S. Electrosynthesis of Phosphacycles via Dehydrogenative C–P Bond Formation Using DABCO as a Mediator. *Org. Lett.* **2021**, *23*, 3120–3124.

(18) Ge, Q.; Zong, J.; Li, B.; Wang, B. Copper-Mediated Annulation of Phosphorus-Containing Arenes with Alkynes: An Approach to Phosphindolium Salts. *Org. Lett.* **2017**, *19*, 6670–6673.

(19) Jin, Y.; Caner, J.; Nishikawa, S.; Toriumi, N.; Iwasawa, N. Catalytic direct hydrocarboxylation of styrenes with CO_2 and H_2. *Nat. Commun.* **2022**, *13*, 7584.

(20) Zhang, T.; Cai, M.; Zhao, W.; Liu, M.; Jiang, N.; Ge, Q.; Cong, H. Electrochemical oxidative intramolecular annulation of aryl phosphine compounds: an efficient approach for synthesizing π-conjugated phosphonium salts. *Green Chem.* **2023**, *25*, 1351–1355.

(21) Cyclization of monovalent phosphorus compounds has been reported. Wei, X.; Lu, Z.; Zhao, X.; Duan, Z.; Mathey, F. Synthesis of Annelated Phospholes through Intramolecular C-H Activation by Monovalent Phosphorus. *Angew. Chem. Int. Ed.* **2015**, *54*, 1583–1586.

(22) Baba, K.; Tobisu, M.; Chatani, N. Palladium-Catalyzed Direct Synthesis of Phosphole Derivatives from Triarylphosphines through Cleavage of Carbon–Hydrogen and Carbon–Phosphorus Bonds. *Angew. Chem. Int. Ed.* **2013**, *52*, 11892–11895.

(23) Masuda, Y.; Tsuda, H.; Murakami, M. Photo-induced Dearomatizing Three-component Coupling of Arylphosphines, Alkenes, and Water. *Angew. Chem. Int. Ed.* **2021**, *60*, 3551-3555.

(24) Masuda, Y.; Ikeshita, D.; Murakami, M. Photocatalytic Cycloaddition Reaction of Triarylphosphines with Alkynes Forming Cyclic Phosphonium Salts. *Chem. Lett.* **2021**, *50*, 1691–1694.

(25) Masuda, Y.; Uno, M.; Murakami, M. Photoinduced Reaction of Triarylphosphines with Alkenes Forming Fused Tricyclic Phosphonium Salts. *Org. Lett.* **2021**, *23*, 8445–8449.

(26) Ikeshita, D.; Masuda, Y.; Ishida, N.; Murakami, M. Photoinduced Hydrophosphination of Terminal Alkynes with Tri(*o*-tolyl)phosphine: Synthesis of Alkenylphosphonium Salts. *Org. Lett.* **2022**, *24*, 2504–2508.

(27) Masuda, Y.; Ikeshita, D.; Higashida, K.; Yoshida, M.; Ishida, N.; Murakami, M.; Sawamura, M. Photocatalytic 1,2-Phosphorus-Migrative [3+2] Cycloaddition of Tri(*t*-butyl)phosphine with Terminal Alkynes. *J. Am. Chem. Soc.* **2023**, *145*, 19060–19066.

(28) Martin, R.; Buchwald, S. L. Palladium-Catalyzed Suzuki–Miyaura Cross-Coupling Reactions Employing Dialkylbiaryl Phosphine Ligands. *Acc. Chem. Res.* **2008**, *41*, 1461–1473.

(29) Slinker, J. D.; Gorodetsky, A. A.; Lowry, M. S.; Wang, J.; Parker, S.; Rohl, R.; Bernhard, S.; Malliaras, G. G. Efficient Yellow Electroluminescence from a Single Layer of a Cyclometalated Iridium Complex. *J. Am. Chem. Soc.* **2004**, *126*, 2763–2767.

(30) Lowry, M. S.; Goldsmith, J. I.; Slinker, J. D.; Rohl, R.; Pascal, R. A.; Malliaras, G. G.; Bernhard, S. Single-Layer Electroluminescent Devices and Photoinduced Hydrogen Production from an Ionic Iridium(III) Complex. *Chem. Mater.* **2005**, *17*, 5712–5719.

(31) Arias-Rotondo, D. M.; McCusker, J. K. The photophysics of photoredox catalysis: a roadmap for catalyst design. *Chem. Soc. Rev.* **2016**, *45*, 5803–5820.

(32) Choi, G. J.; Zhu, Q.; Miller, D. C.; Gu, C. J.; Knowles, R. R. Catalytic alkylation of remote C–H bonds enabled by proton-coupled electron transfer. *Nature* **2016**, *539*, 268–271.

(33) Nishida, J. I.; Kawakami, Y.; Yamamoto, S.; Matsui, Y.; Ikeda, H.; Hirao, Y.; Kawase, T. Synthesis and photophysical studies of dibenzophosphole oxides with D–A–D triad structures. *Eur. J. Org. Chem.* **2019**, *2019*, 3735–3743.

(34) Stambuli, J. P.; Stauffer, S. R.; Shaughnessy, K. H.; Hartwig, J. F. Screening of Homogeneous Catalysts by Fluorescence Resonance Energy Transfer. Identification of Catalysts for Room-Temperature Heck Reactions. *J. Am. Chem. Soc.* **2001**, *123*, 2677–2678.

(35) Martin, R. L.; Hay, P. J.; Pratt, L. R. Hydrolysis of Ferric Ion in Water and Conformational Equilibrium. *J. Phys. Chem. A* **1998**, *102*, 3565–3573.

(36) For selected reviews on photocatalytic generation of phosphine radical cations, see: (a) Rossi-Ashton, J. A.; Clarke, A. K.; Unsworth, W. P.; Taylor, R. J. K. Phosphoranyl Radical Fragmentation Reactions Driven by Photoredox Catalysis. *ACS Catal.* **2020**, *10*, 7250–7261. (b) Pan, D.; Nie, G.; Jiang, S.; Li, T.; Jin, Z. Radical reactions promoted by trivalent tertiary phosphines. *Org. Chem. Front.* **2020**, *7*, 2349–2371.

(37) See Supporting Information for noncovalent interaction analysis for the van der Waals complex **2a**···*t*-Bu• with the IGMH method in the Multiwfn program.

(38) For the reported example of a van der Waals complex consisting of radical fragments, see: Ueda, Y.; Masuda, Y.; Iwai, T.; Imaeda, K.; Takeuchi, H.; Ueno, K.; Gao, M.; Hasegawa, J.; Sawamura, M. Photoinduced Copper-Catalyzed Asymmetric Acylation of Allylic Phosphates with Acylsilanes. *J. Am. Chem. Soc.* **2022**, *144*, 2218–2224. See also ref 27.

(39) Cismesia, M. A.; Yoon, T. P. Characterizing chain processes in visible light photoredox catalysis. *Chem. Sci.* **2015**, *6*, 5426–5434.

(40) de Pedro Beato, E.; Mazzarella, D.; Balletti, M.; Melchiorre, P. Photochemical generation of acyl and carbamoyl radicals using a nucleophilic organic catalyst: applications and mechanism thereof. *Chem. Sci.* **2020**, *11*, 6312–6324.

(41) Koga, N.; Morokuma, K. Determination of the lowest energy point on the crossing seam between two potential surfaces using the energy gradient. *Chem. Phys. Lett.* **1985**, *119*, 371–374.

(42) Bernardi, F.; Olivucci, M.; Robb, M. A. Potential energy surface crossings in organic photochemistry. *Chem. Soc. Rev.* **1996**, *25*, 321–328.

(43) Yarkony, D. R. Diabolical conical intersections. *Rev. Mod. Phys.* **1996**, *68*, 985–1013.

(44) Harvey, J. N.; Aschi, M.; Schwarz, H.; Koch, W. The singlet and triplet states of phenyl cation. A hybrid approach for locating minimum energy crossing points between non-interacting potential energy surfaces. *Theor. Chem. Acc.* **1998**, *99*, 95–99.

(45) Yarkony, D. R. Conical Intersections: Diabolical and Often Misunderstood. *Acc. Chem. Res.* **1998**, *31*, 511–518.

(46) Harvey, J. N.; Aschi, M. Spin-forbidden dehydrogenation of methoxy cation: a statistical view. *Phys. Chem. Chem. Phys.* **1999**, *1*, 5555–5563.

(47) Sobolewski, A. L.; Domcke, W.; Dedonder-Lardeux, C.; Jouvet, C. Excited-state hydrogen detachment and hydrogen transfer driven by repulsive $^1\pi\sigma^*$ states: A new paradigm for nonradiative decay in aromatic biomolecules. *Phys. Chem. Chem. Phys.* **2002**, *4*, 1093–1100.

(48) Lewis, P. J.; Bennett, K. A.; Harvey, J. N. A computational study of the atmospheric oxidation of nopinone. *Phys. Chem. Chem. Phys.* **2005**, *7*, 1643–1649.

(49) Nanbu, S.; Ishida, T.; Nakamura, H. Future perspectives of nonadiabatic chemical dynamics. *Chem. Sci.* **2010**, *1*, 663–674.

(50) Marcus, R. A. On the Theory of Oxidation‐Reduction Reactions Involving Electron Transfer. I. *J. Chem. Phys.* **1956**, *24*, 966–978.

(51) Marcus, R. A. Electron Transfer Reactions in Chemistry: Theory and Experiment (Nobel Lecture). *Angew. Chem. Int. Ed.* **1993**, *32*, 1111–1121.

(52) Poli, R.; Harvey, J. N. Spin forbidden chemical reactions of transition metal compounds. New ideas and new computational challenges. *Chem. Soc. Rev.* **2003**, *32*, 1–8.

(53) Harvey, J. N. Understanding the kinetics of spin-forbidden chemical reactions. *Phys. Chem. Chem. Phys.* **2007**, *9*, 331–343.

(54) Harvey, J. N. Spin-forbidden reactions: computational insight into mechanisms and kinetics. *WIREs Comput. Mol. Sci.* **2014**, *4*, 1–14.

(55) Gaggioli, C. A.; Belpassi, L.; Tarantelli, F.; Harvey, J. N.; Belanzoni, P. Spin-Forbidden Reactions: Adiabatic Transition States Using Spin–Orbit Coupled Density Functional Theory. *Chem. Eur. J.* **2018**, *24*, 5006–5015.

(56) Harabuchi, Y.; Hayashi, H.; Takano, H.; Mita, T.; Maeda, S. Oxidation and Reduction Pathways in the Knowles Hydroamination via a Photoredox-Catalyzed Radical Reaction. *Angew. Chem. Int. Ed.* **2023**, *62*, e202211936.

(57) Hatanaka, M.; Morokuma, K. Exploring the Reaction Coordinates for f–f Emission and Quenching of Lanthanide Complexes – Thermosensitivity of Terbium(III) Luminescence. *J. Chem. Theory Comput.* **2014**, 10, 4184–4188.

(58) Hatanaka, M.; Hirai, Y.; Kitagawa, Y.; Nakanishi, T.; Hasegawa, Y.; Morokuma, K. Organic Linkers Control the Thermosensitivity of the Emission Intensities from Tb(III) and Eu(III) in a Chameleon Polymer. *Chem. Sci.* **2017**, 8, 423–429.

(59) Maeda, S.; Harabuchi, Y.; Sumiya, Y.; Takagi, M.; Suzuki, K.; Sugiyama, K.; Ono, Y.; Hatanaka, M.; Osada, Y.; Taketsugu, T.; Morokuma, K.; Ohno, K. GRRM23, 2023. https://global.hpc.co.jp/products/grrm23/ (March 10, 2025).

(60) According to the calculations, hydrogen atom transfer from intermediate **B** to *t*-Bu• was expected to be another feasible radical termination pathway (an activation energy of 1.7 kcal mol^{-1}), affording **3a** and *t*-Bu–H.

(61) Lin, Q.-Y.; Xu, X.-H.; Qing, F.-L.; Zhang, K.; Qing, F.-L. Visible-Light-Induced Hydrodifluoromethylation of Alkenes with a Bromodifluoromethylphosphonium Bromide. *Angew. Chem. Int. Ed.* **2016**, *55*, 1479–1483.

(62) Panferova, L. I.; Tsymbal, A. V.; Levin, V. V.; Struchkova, M. I.; Dilman, A. D. Reactions of *gem*-Difluorinated Phosphonium Salts Induced by Light. *Org. Lett.* **2016**, *18*, 996–999.

(63) Ran, Y.; Lin, Q.-Y.; Xu, X.-H.; Qing, F.-L. Visible Light Induced Oxydifluoromethylation of Styrenes with Difluoromethyltriphenylphosphonium Bromide. *J. Org. Chem.* **2016**, *81*, 7001–7007.

(64) Miura, T.; Funakoshi, Y.; Nakahashi, J.; Moriyama, D.; Murakami, M. Synthesis of Elongated Esters from Alkenes. *Angew. Chem. Int. Ed.*, **2018**, *57*, 15455–15459.

(65) Miura, T.; Moriyama, D.; Funakoshi, Y.; Murakami, M. Photoinduced 1,2-Hydro(cyanomethylation) of Alkenes with a Cyanomethylphosphonium Ylide. *Synlett* **2019**, *30*, 511–514.

(66) Miura, T.; Moriyama, D.; Miyakawa, S.; Murakami, M. Synthesis of Alkyl Sulfones from Alkenes and Tosylmethylphosphonium Iodide through Photo-Promoted C-C Bond Formation. *Chem. Lett.* **2020**, *49*, 1382–1385.

(67) Matsumoto, A.; Maeda, N.; Maruoka, K. Bidirectional Elongation Strategy Using Ambiphilic Radical Linchpin for Modular Access to 1,4-Dicarbonyls via Sequential Photocatalysis. *J. Am. Chem. Soc.* **2023**, *145*, 20344–20354.

(68) In the case of **Ir3**, its excited state can also reduce **3a-BF$_4$** (Ir(III)*/(IV) = -1.73 V).

TOC Graphic

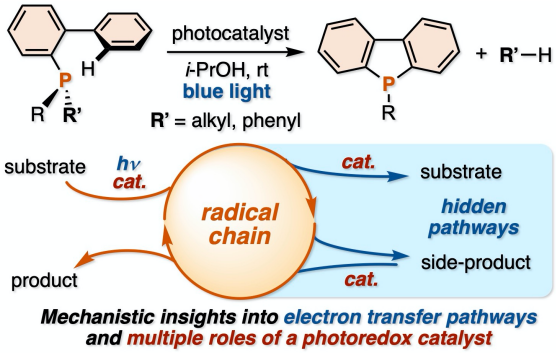
photocatalyst
i-PrOH, rt
blue light
R' = alkyl, phenyl
+ R'—H
substrate
hν
cat.
radical
chain
product
cat.
substrate
hidden
pathways
side-product
cat.
Mechanistic insights into electron transfer pathways
and multiple roles of a photoredox catalyst